

## [ Imaging ]

# Imaging of Sports-Related Midfoot and Forefoot Injuries

Alissa J. Burge, MD,\* Stephanie L. Gold, BA,\* and Hollis G. Potter, MD\*†

Sports-related injuries of the foot are common and may result in significant morbidity, particularly if inaccurate or delayed diagnosis leads to improper management. While less common than injuries of the ankle, sports-related foot injuries account for 2% to 18% of athletic injuries. Injury may occur as a result of acute trauma or chronic overuse, and high-impact sports that involve running, jumping, or contact place the athlete at higher risk for injury. Accurate and timely diagnosis of injury is the key to proper management, and diagnostic imaging studies often play a critical role in this regard. While radiographs, computerized tomography scans, and ultrasound are useful in the evaluation of the foot, magnetic resonance imaging provides superior tissue contrast as well as the ability to detect stress reaction in bone that precedes discernible fracture line on radiographs, allowing accurate detection of both osseous and soft tissue pathology. This review focuses on imaging of common sports-related injuries of the midfoot and forefoot, including osseous, ligamentous, and tendinous pathology, with emphasis on magnetic resonance imaging diagnosis.

**Keywords:** imaging; magnetic resonance imaging; sports; injuries; foot

Sports-related injuries of the foot are common and may result in significant morbidity, particularly if inaccurate or delayed diagnosis leads to improper management.<sup>1,6,29</sup> Such injuries account for approximately 2% to 18% of athletic injuries, depending on the type of activity, with sports involving running, jumping, and contact resulting in greater risk of injury. Foot injuries constitute approximately 2% of football, basketball, and women's soccer injuries; 4% of men's soccer injuries; and up to 18% of martial arts injuries.<sup>2,8,12,34</sup> Altered anatomy resulting in altered biomechanics, such as hallux valgus and congenitally elongated second toe, may also result in a predisposition toward the development of athletic foot injuries.<sup>14</sup>

The complex anatomy of the foot is critical in allowing it to support the weight of the body over a range of activities. During quiet standing, the foot functions as a mobile adaptor, with the medial longitudinal arch passively supported by the ligaments and plantar fascia and with little contribution from the muscles. During propulsion, however, the foot changes shape, becoming rigid, with tightening of the plantar aponeurosis and significant contribution from muscle activity, particularly the tibialis anterior, tibialis posterior, and peroneus longus. Each portion of the foot experiences variable loads during activity, with structures such as the great toe, first metatarsal head, and heel commonly experiencing relatively more stress due to their

critical supportive functions. Movements commonly performed during sports, such as running, cutting, jumping, and landing, result in even greater stresses upon the critical supportive structures of the foot.<sup>25,31</sup>

Radiographs are often utilized as an initial imaging examination in the setting of athletic injury, but they provide limited sensitivity for soft tissue and subtle osseous injuries; however, acquiring weightbearing views as well as images of the contralateral foot aids in the identification of subtle alterations in alignment indicative of soft tissue injury. Fluoroscopy provides the ability to dynamically image osseous structures, allowing dynamic stress views in real time, particularly useful in assessing instability. Computed tomography provides excellent evaluation of osseous morphology, but evaluation of the soft tissues remains limited, and the use of ionizing radiation is an additional concern. Ultrasound has been established as an effective method of imaging soft tissue injury, particularly of the ligaments and tendons, and has the additional ability to provide dynamic evaluation of structures in motion, but it provides relatively insensitive evaluation of osseous pathology. Magnetic resonance imaging (MRI), by virtue of a combination of superior tissue contrast and the ability to detect marrow edema, provides accurate, sensitive evaluation of soft tissue and osseous injuries.

From the \*Hospital for Special Surgery, New York, New York

†Address correspondence to Hollis Potter, MD, Hospital for Special Surgery, 535 East 70th Street, New York, NY 10021 (e-mail: potterh@hss.edu).

Hollis G. Potter is a board member at Kensey Nash Corp.; a consultant for Biomet, BioMimetic Therapeutics, Smith & Nephew, Kensey Nash Corp., Histogenics Corp, and Stryker; received financial support from Depuy Orthopaedics, Vindico, and General Electric Healthcare; and received grants from NIH NIAMS Challenge (RC1AR058255-01) and NIH/NIMAS (1R01AR057343-01A2)

DOI: 10.1177/1941738112459489

© 2012 The Author(s)

	Coronal fast inversion recovery	Axial FSE	Sagittal FSE	Coronal FSE	Thin Sagittal FSE
TR (msec)	4000-4500	5000	4000	4000	4000
TE (msec)	17	32	32	32	32
TI	150	na	na	na	na
BW (kHz)	31.25	31.25	31.25	31.25	31.25
ETL	7 – 10	7 – 12	7-12	7 – 12	7-12
Flip (degr)	na	na	na	na	na
NEX	2	2	2	3	2
FOV (cm)	16	10	13-15	12	15
Matrix	256 x 192	512 x 320	512 x 256	512 x 320 – 352	512x320
Slice/gap (mm)	3/0	3/0	4/0	2/0	1.5/0
NPW	Y	Y	Y	Y	Y
Frequency	R/L	A/P	Swap	R/L	Swap

Figure 1. Recommended protocols for imaging the foot at 1.5 T. TR = time to repetition; TE = time to echo; TI = time to inversion; BW = bandwidth; ETL = echo train length; Flip = flip angle; NEX = number of excitations; FOV = field of view; NPW = no phase wrap.

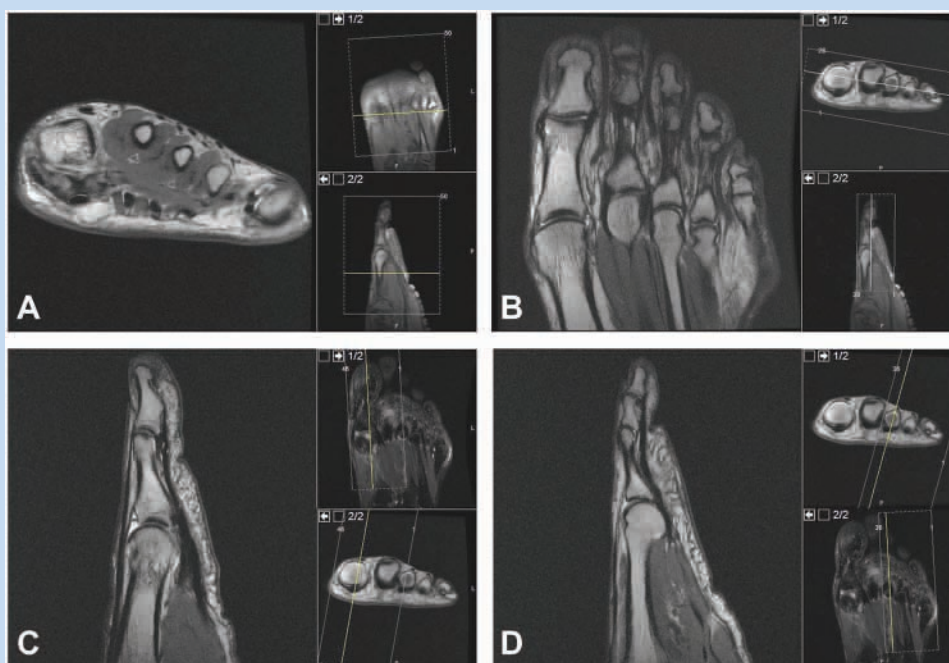


Figure 2. Imaging planes of the forefoot: axial (A), oblique coronal (B), sagittal through first ray (C), and sagittal through lesser rays (D).

MRI of the foot is best performed utilizing a dedicated extremity coil at 1.5 or 3.0 T. Oblique coronal fast inversion recovery and 3-plane intermediate echo-time fast-spin echo (FSE) sequences performed along the anatomic axes of the foot and centered on the midfoot or forefoot as clinically indicated allow thorough evaluation of osseous structures, cartilage, and soft tissues, with additional sequences performed as needed (Figures 1 and 2). Within the forefoot, the addition of a thin sagittal FSE sequence through the first ray augments evaluation of the complex anatomy of the first metatarsophalangeal (MTP) joint, particularly in the setting of a hallux valgus when

the sagittal ankle of the first metatarsal deviates from the remaining portion of the foot.

## **PATHOLOGY**

### **Lisfranc Joint Injury**

Injuries at the tarsometatarsal, or Lisfranc, joint may occur in the setting of either high- or low-velocity trauma. High-velocity injuries are typically sustained in the setting of trauma associated with motor vehicle collisions or falls from a height.<sup>13</sup> Sports-related injuries of the Lisfranc joint are generally

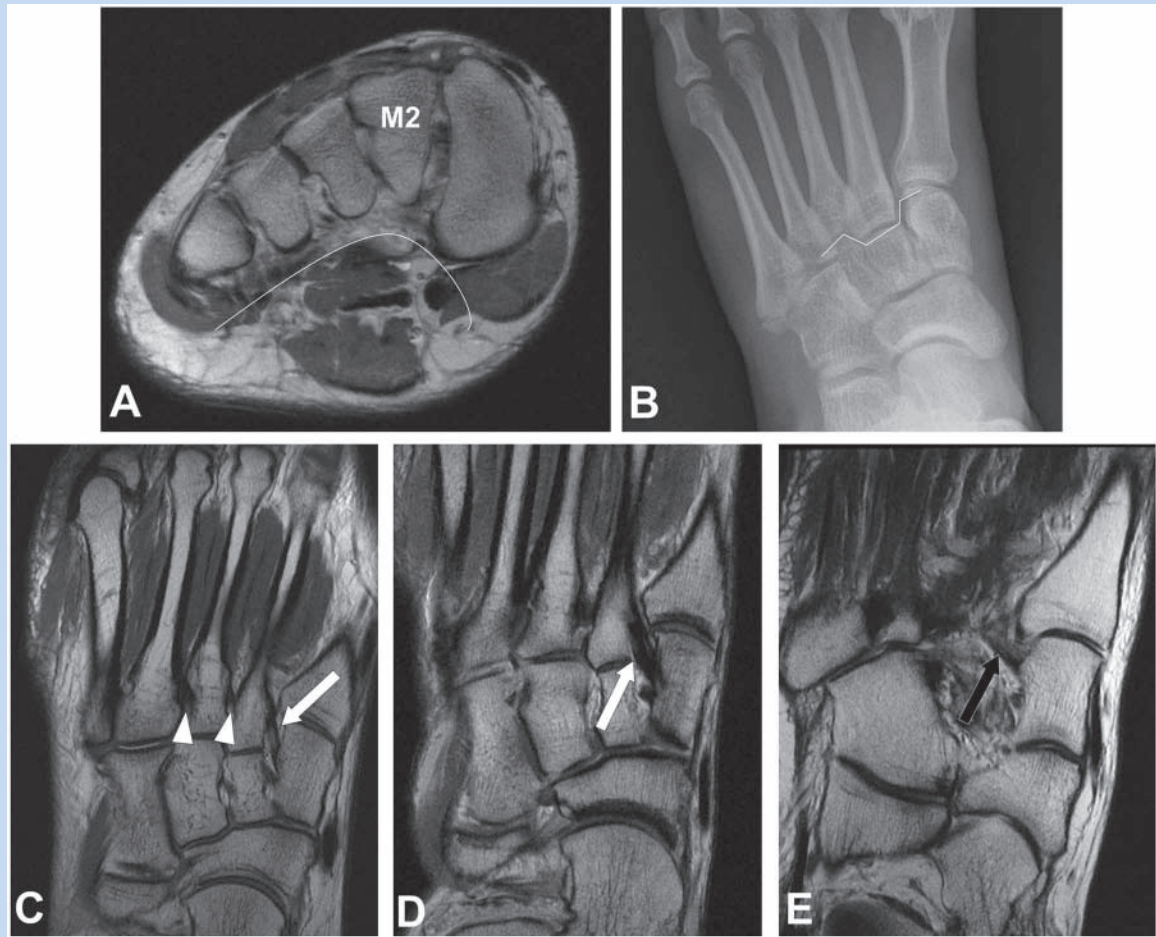


Figure 3. Axial FSE at the level of a normal Lisfranc joint (A) demonstrates asymmetric arch configuration of the osseous structures, with the second metatarsal base (M2) as the keystone. Anteroposterior radiograph of the foot (B) demonstrates mortise configuration at the tarsometatarsal joint, as the second metatarsal base is recessed between the medial and lateral cuneiforms. Coronal FSE images of the midfoot (C-E) demonstrate the dorsal (white arrow) and plantar (black arrow) bands of the Lisfranc ligament, as well as the second and third intermetatarsal ligaments (white arrowhead).

considered low velocity, occurring during forced plantar flexion. Situations predisposing an athlete to this type of injury include certain stances, such as the lineman's blocking stance in American football, in which the foot is plantar flexed and the MTP joint is dorsiflexed, as well as activities involving the use of foot straps, such as surfing and horseback riding.<sup>36</sup> In the first situation, a force directed downward onto the heel, such as that generated by a tackle or falling player, results in hyperplantarflexion of the Lisfranc joint. In the second, hyperplantarflexion occurs because of a backward fall with entrapment of the forefoot within the foot strap, as initially described by Napoleon's field surgeon, Jacques Lisfranc, in his observation of stirrup injuries during the Napoleonic war.<sup>17</sup>

The Lisfranc joint consists of the articulation between the cuboid and 3 cuneiforms proximally and the bases of the 5 metatarsals distally. The stability of the Lisfranc joint is derived from osseous relationships and ligamentous support.

The position of the second metatarsal base is an essential component of osseous stability. In short axis, the osseous structures at the Lisfranc articulation form an arch, with the second metatarsal, due to its dorsal-most position, forming the keystone of the arch (Figure 3A). In the long axis, the second metatarsal base is recessed between the medial and lateral cuneiforms, forming a mortise (Figure 3B). Numerous ligaments stabilize the tarsometatarsal articulation, the strongest being the Lisfranc ligament proper, which bridges the interval between the medial cuneiform and the base of the second metatarsal and consists of plantar and dorsal fibers (Figure 3C-3E). The remaining ligamentous restraints may be divided into plantar, dorsal, and interosseous components, spanning the intertarsal, intermetatarsal, and tarsometatarsal articulations.<sup>6,11,13</sup>

On MRI, the normal Lisfranc ligament appears as low-signal-intensity dorsal and plantar bands, which are well visualized in the coronal and axial planes. The dorsal and plantar capsular

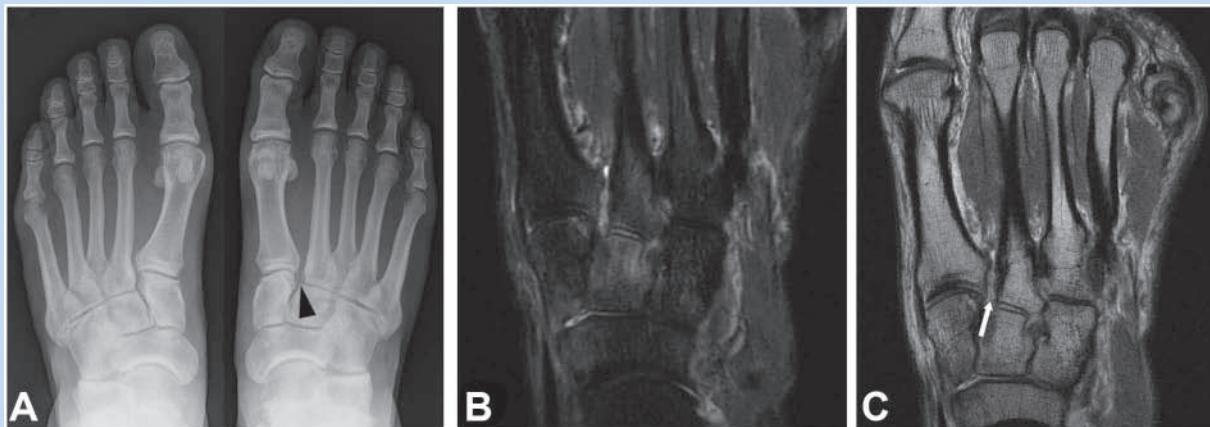


Figure 4. Thirty-four-year-old man with isolated Lisfranc ligament injury following plantar flexion football injury. Radiographs of the bilateral feet (A) demonstrate widening of the right Lisfranc interval (black arrowhead). Coronal short tau inversion recovery of the midfoot (B) demonstrates marrow edema signal within the medial and middle cuneiforms and first and second metatarsal bases, with hyperintense signal in the Lisfranc interval. Coronal FSE of the midfoot (C) demonstrates disruption of the dorsal fibers of the Lisfranc ligament (white arrow).

ligamentous restraints are better assessed in the sagittal and axial planes.

Lisfranc injury may range from isolated ligamentous sprain to complete disruption of the tarsometatarsal articulation. Radiographic assessment of isolated Lisfranc ligament injury may demonstrate widening of the Lisfranc interval (Figure 4A).<sup>6,13,17</sup> On MRI, acute ligamentous injury appears as alterations in normal ligament signal and morphology. The ligament may experience interstitial load without failing, in which case the fibers may appear hyperintense and thickened but not discontinuous, indicative of plastic deformation. As the Lisfranc ligament helps to support the longitudinal arch, failure to recognize soft tissue failure may result in rapidly progressive osteoarthritis of the midfoot. Tears of the ligament appear as disruption of ligament fibers with associated local soft tissue and bone marrow edema; disruption of either the dorsal or plantar band of the ligament constitutes a partial tear, while disruption of both bands is designated a complete tear. Potter et al<sup>27</sup> established the utility of MRI for the assessment of Lisfranc injury in a series of athletes who had sustained acute midfoot injuries, demonstrating high accuracy upon radiographic and surgical correlation and confirming prior reports that the weaker dorsal fibers of the ligament are more commonly torn than the more robust plantar fibers in the setting of partial thickness injury (Figure 4B and 4C).<sup>24</sup> Raikin et al<sup>29</sup> demonstrated that disruption of the plantar fibers of the Lisfranc ligament on imaging provides a predictor of Lisfranc joint instability, with a positive predictive value of 94%, allowing accurate determination of the need for surgical intervention.

As the extent of ligamentous disruption at the tarsometatarsal articulation progresses beyond isolated single-ligament injury, varying patterns of osseous displacement may be observed, as addressed by the multiple classification systems that have

evolved over the years to describe these injuries. Classically, 3 patterns of displacement were described: homolateral, in which all 5 metatarsals are displaced in the same direction; divergent, in which the first metatarsal is displaced in the opposite direction from metatarsals 2 to 5; and isolated, in which some of the metatarsals are spared.<sup>13</sup> More comprehensive systems based on the same general principle of displacement have been described, with Myerson et al<sup>24</sup> dividing these injuries into 3 main categories (total incongruity, partial incongruity, and divergent), within which various subtypes exist; these authors also favor the term “tarsometatarsal joint complex” over the designation “Lisfranc” or “tarsometatarsal” joint, in recognition of the fact that these injuries may also involve the intercuneiform and naviculocuneiform articulations.<sup>24,36</sup> These injuries are often associated with fractures (up to 90%), which commonly involve the plantar medial aspect of the second metatarsal base or the distal lateral aspect of the middle cuneiform. Careful scrutiny of the capsular ligaments of the first tarsometatarsal joint is important, as failure to recognize instability at this joint may result in rapidly progressive osteoarthritis following isolated surgical stabilization of the Lisfranc interval (Figure 5).<sup>27</sup>

### Ligament and Tendon Injuries

*Long medial flexors.* Posterior tibial tendon (PTT) pathology may be the result of both acute and long-standing processes, but it is most commonly related to chronic attritional change due to cumulative daily stresses and overuse, gradually evolving from tenosynovitis to tendinosis to partial tears. At and distal to the medial malleolus, the PTT is relatively hypovascular and therefore more prone to injury in this region. Additionally, altered biomechanics, as seen in the setting of

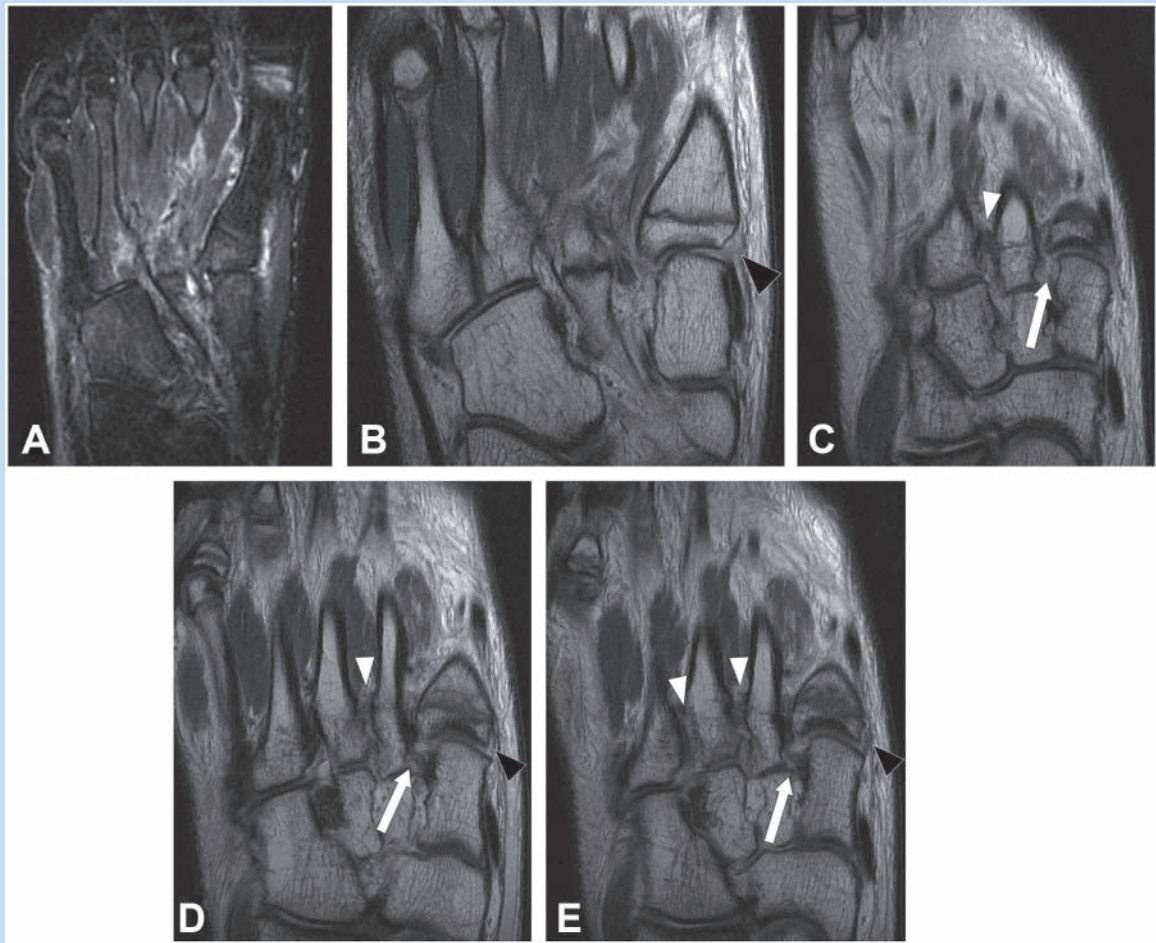


Figure 5. Fifteen-year-old boy with Lisfranc fracture-dislocation following sports-related midfoot injury. Coronal short tau inversion recovery (A) images demonstrates soft tissue edema within the midfoot and marrow edema pattern within the fourth metatarsal base. Coronal proton density images (B-E) demonstrate complete disruption of the Lisfranc ligament (white arrows), as well as complete disruption of the second intermetatarsal ligament and partial disruption of the third (white arrowheads). Additionally, there is disruption of the capsular ligaments of the first tarsometatarsal joint (black arrowhead), with resultant lateral subluxation of the first metatarsal base.

gait abnormalities, and anatomic variants, such as accessory ossicles, may result in a predisposition to PTT injury.<sup>32</sup> Because of the critical supportive function of the PTT in maintaining the medial longitudinal arch of the foot, PTT insufficiency commonly leads to secondary acquired flatfoot deformity.<sup>7,32</sup> Acute PTT tears are rare and, in contrast to chronic tears, typically occur at the navicular insertion, with more proximal overload seen in running athletes.<sup>5</sup> More commonly, acute PTT pathology consists of a tenosynovitis related to acute overuse in athletes, particularly those participating in sports requiring rapid changes in direction, such as basketball, hockey, and soccer.<sup>32</sup> Injury of the remaining long medial flexors is relatively uncommon, though flexor hallucis longus pathology has been recognized as occurring with elevated frequency in ballet dancers, due to the repetitive stresses placed on the tendon when dancing en pointe.<sup>18</sup>

The tibialis posterior muscle arises within the calf, originating from the posterior aspects of the tibia, interosseous ligament, and fibula, and becoming tendinous just above the ankle, where it courses distally along the medial aspect of the ankle to its insertion points upon the navicular, cuneiforms, and metatarsals. Along with the spring ligament and tibialis anterior, the PTT plays a critical role in maintaining the normal medial longitudinal arch of the foot.<sup>22</sup>

The proximal long medial flexor tendons are well visualized in the axial plane of the ankle; more distally, as the tendons change course, they are better evaluated in the axial plane as prescribed relative to the foot. The long medial flexors are also well evaluated on ultrasound, upon which the normal tendons appear as relatively hyperechoic structures consisting of longitudinally oriented parallel hyperechoic lines. Imaging findings of PTT injury depend on the type and severity of



Figure 6. Forty-five-year-old runner with PTT insufficiency and secondary flatfoot deformity. Coronal (A) and axial (B) FSE images demonstrate marked thickening and hyperintensity of the PTT (white arrows), related to severe tendinosis. Weightbearing radiograph (C) demonstrates severe secondary flatfoot deformity.

pathology; for example, an acute tenosynovitis incited by athletic overuse manifests as simple fluid within the tendon sheath. Chronic disease commonly begins as a tenosynovitis, often with adhesions and synechiae within the tendon sheath, and progresses to tendinosis and, subsequently, partial-thickness tears. Imaging manifestations of resultant secondary flatfoot deformity include flattening of the medial longitudinal arch (best quantified on weightbearing radiographs), hindfoot valgus, talocalcaneal impaction, and, if long-standing and severe, subfibular impingement (Figure 6).<sup>30,32</sup> The presence of an accessory navicular may also predispose to pathology, serving as a risk factor for PTT tendon degeneration and/or tear or, if a type 2 accessory navicular, to the development of stress reaction about the synchondrosis (Figure 7).

**Spring ligament.** Spring ligament pathology is rarely related to acute injury and is generally associated with deficiency of structures that serve a similar biomechanical function, particularly the PTT. Because spring ligament pathology

typically occurs in association with, and is generally preceded by, PTT degeneration, the clinical manifestations and ancillary findings are similar.<sup>32</sup>

The spring ligament consists of 3 components: the superomedial, medioplantar oblique, and the inferoplantar longitudinal bands. The superomedial band, which is the strongest, originates on the sustentaculum tali and tibiospring component of the deltoid, and inserts on the superomedial aspect of the navicular. The remaining 2 bands originate from the coronoid fossa of the calcaneus, with the medioplantar oblique inserting on the navicular tuberosity and with the inferoplantar longitudinal inserting upon the navicular beak.<sup>23</sup> As mentioned previously, the spring ligament serves a critical supportive function in maintaining the medial longitudinal arch of the foot, along with the PTT and tibialis anterior.<sup>7,22,23,32</sup>

The spring ligament is best visualized in the axial and coronal planes (Figure 8A and 8B). Primary imaging manifestations of spring ligament pathology include abnormal thickening, hyperintensity, attenuation, and/

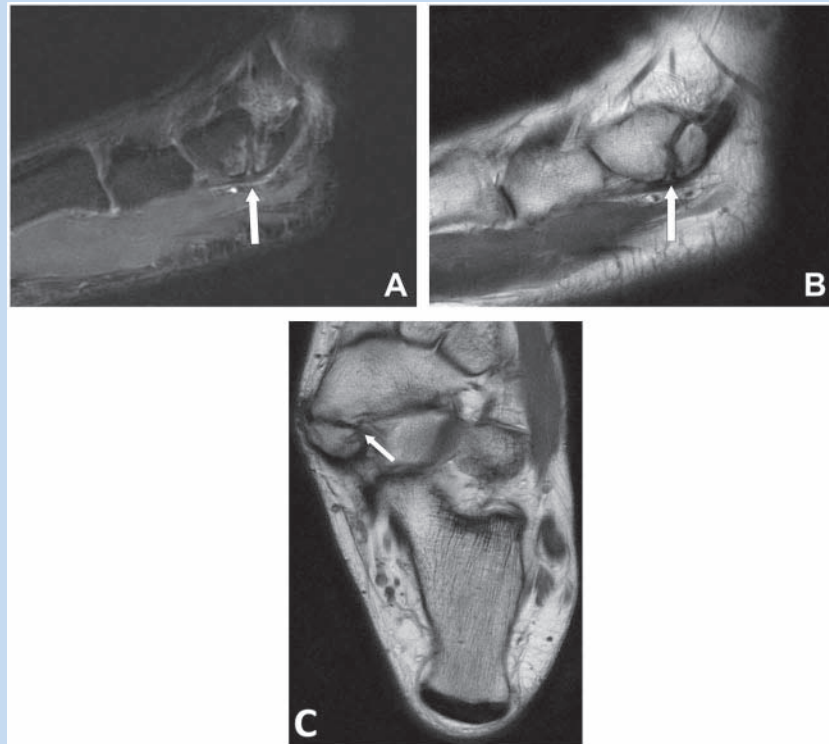


Figure 7. Twenty-six-year-old basketball player with stress reaction about the synchondrosis of a type 2 accessory navicular. Sagittal short tau inversion recovery (A) demonstrates marrow edema on both sides of the synchondrosis of a large type 2 accessory navicular (white arrow). Sagittal (B) and coronal (C) FSE images demonstrate irregularity and sclerosis about the synchondrosis (white arrows).

or disruption of ligament fibers (Figure 8C). As with PTT dysfunction, secondary imaging signs reflect the biomechanical consequences of deficient medial longitudinal arch support, with acquired flatfoot deformity, hindfoot valgus, tibiocalcaneal impingement, and subfibular impingement. Concomitant deficiency of the PTT is essentially universal.<sup>22,23,32</sup> In addition to facilitating anatomic delineation, the injection of intra-articular gadolinium may demonstrate areas of ligamentous discontinuity, which should be differentiated from a “spring ligament recess,” a synovium-lined recess in contiguity with the talonavicular joint, seen in association with hindfoot and midfoot pathology yielding talonavicular joint effusion; on imaging, this teardrop-shaped recess is characterized by well-defined borders, homogeneous fluid signal, and a neck extending from the talonavicular joint, insinuating between the medioplantar oblique and inferoplantar longitudinal components of the spring ligament.<sup>9,20</sup>

*Anterior extensor tendons.* The tibialis anterior tendon inserts upon the inferomedial aspect of the first metatarsal base and the anteromedial aspect of the medial cuneiform, serving as an additional support of the medial longitudinal arch. Although relatively rare, spontaneous rupture of the tibialis anterior has been reported in association with underlying systemic diseases

such as gout, rheumatoid arthritis, and diabetes mellitus. Acute extensor injury is typically related to direct trauma to the tendon, such as laceration and is not commonly encountered in athletic injuries.<sup>21,32</sup>

In the uncommon case of spontaneous rupture, disruption typically occurs at the level of the ankle joint; rupture at the level of the distal insertion is rare. The torn tendon stump commonly retracts above the level of the ankle joint. Extensor disruption at the level of the foot is more commonly related to direct trauma, with associated imaging findings related to the type and mechanism of injury; tibialis anterior rupture may commonly occur in the setting of laceration, massive trauma, and fractures (Figure 9).<sup>15,21</sup>

*Peroneal tendons.* Injury to the peroneal tendons often occurs in the setting of acute or chronic lateral ligament tears and is relatively common. Risk factors for rupture include preexisting degeneration, lateral ligament insufficiency, and the presence of an os peroneum, which may contribute to degeneration of the peroneus longus tendon. Peroneus brevis split may occur acutely or chronically, and the peroneus longus tendon commonly insinuates within the split, preventing healing.<sup>16,32</sup>

Isolated tears of the peroneus longus typically occur at the level of the midfoot, in the region of the cuboid tunnel

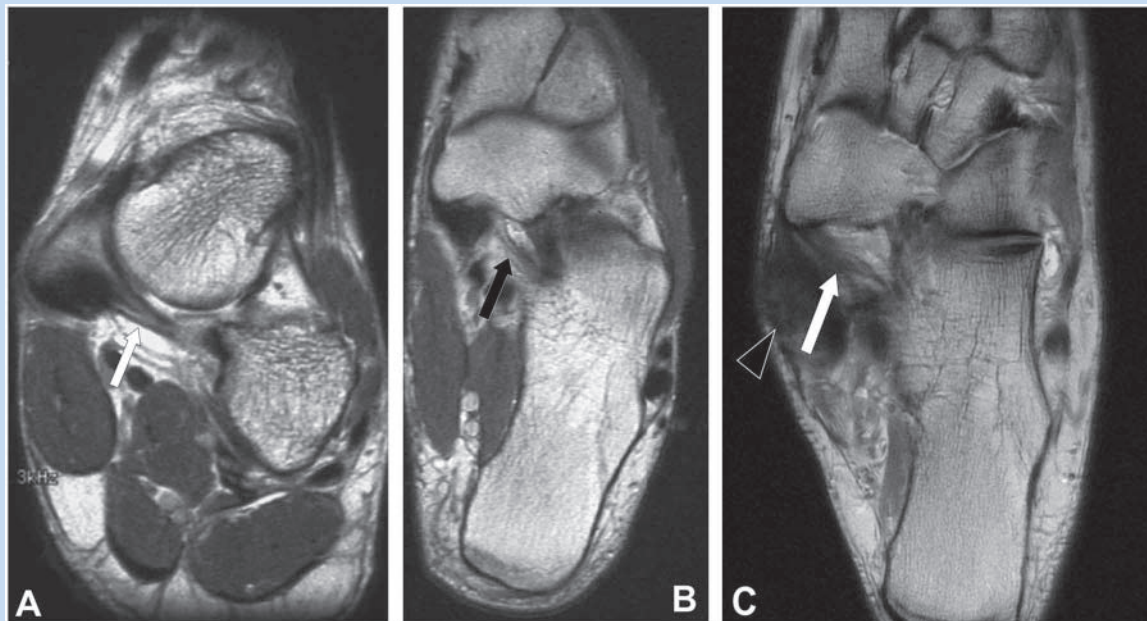


Figure 8. Spring ligament. Axial (A) and coronal (B) FSE images demonstrate the superomedial (white arrow) and medioplantar oblique (black arrow) bands of the normal spring ligament. Coronal FSE image (C) in a 45-year-old runner with secondary flatfoot deformity demonstrates severe tendinosis of the PTT (black arrowhead) with associated deficiency of the spring ligament (white arrow), which is attenuated.

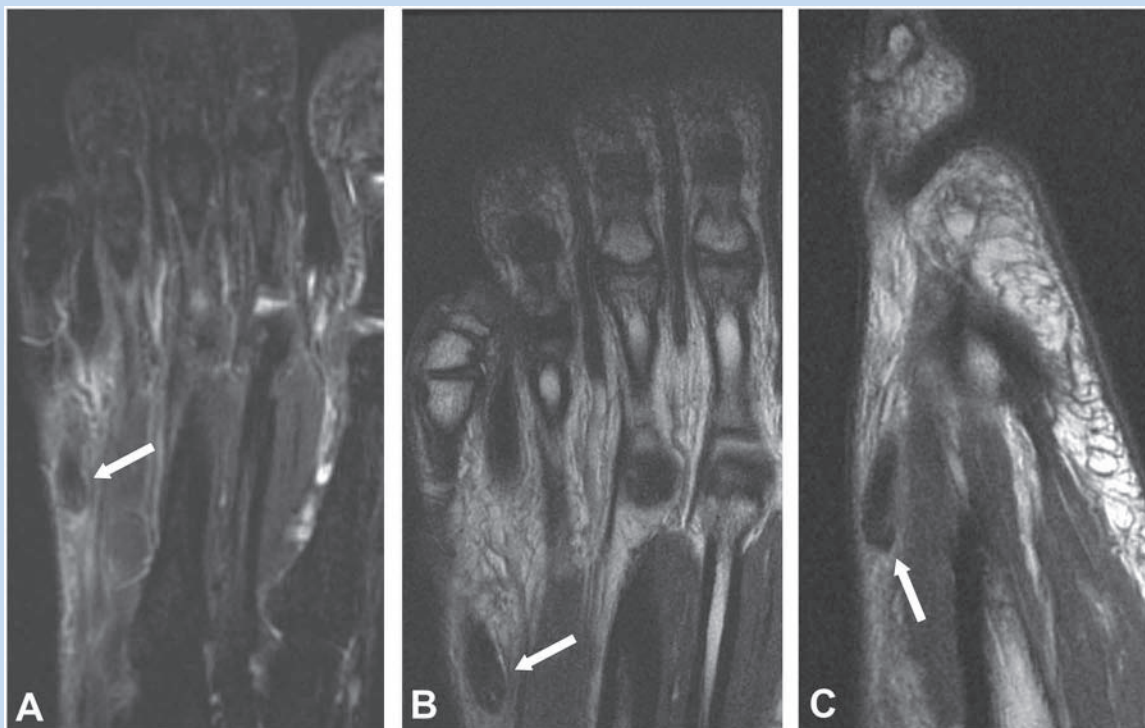


Figure 9. Thirty-year-old diver with traumatic disruption of extensor digitorum tendon. Coronal short tau inversion recovery (A), FSE (B), and sagittal FSE (C) images demonstrate complete disruption of the extensor digitorum tendon to the small digit, with thickening and hyperintensity of the distal stump (white arrows).



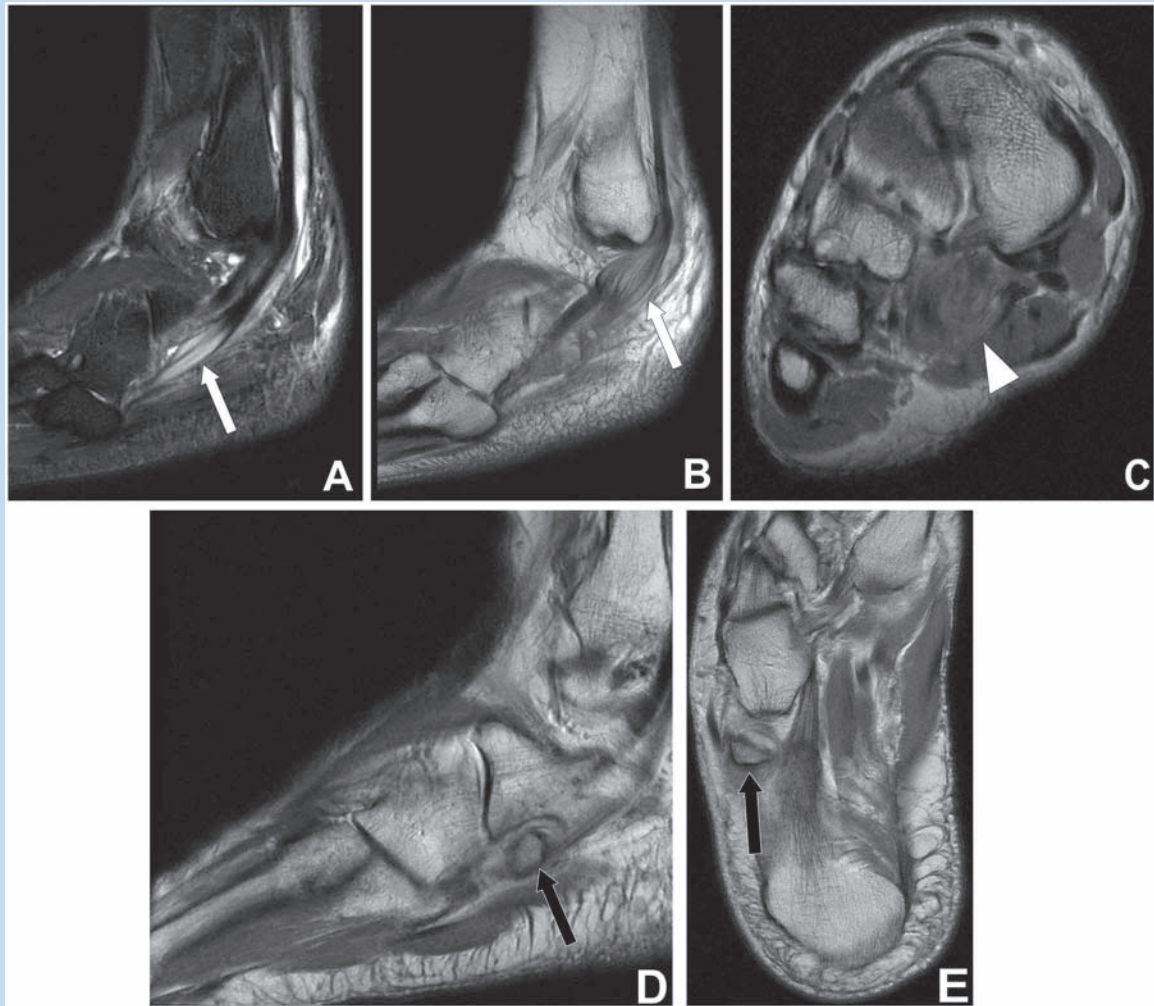


Figure 10. Peroneal tendon injuries. Sagittal short tau inversion recovery (A) and FSE (B) images in a 34-year-old basketball player demonstrate complex splits of both peroneal tendons (white arrows). Axial FSE (C) in a 60-year-old tennis player demonstrates pseudomass (white arrowhead) related to rupture of peroneus longus tendon at the level of the midfoot. Sagittal (D) and coronal (E) FSE images in a 35-year-old soccer player demonstrate rupture of the peroneus longus resulting in proximal retraction of an os peroneum (black arrows).

(Figure 10A-10C). Rupture at this level in the presence of an os peroneum may result in proximal retraction of the os to the level of the calcaneocuboid joint and may therefore be evident on radiographs (Figure 10D and 10E). Chronic stress injury involving an os peroneum may manifest with marrow edema, fragmentation, and sclerosis of the ossicle, as well as degeneration of the surrounding peroneus longus tendon.<sup>32</sup> Pes cavovarus, classically described as a result of neuromuscular imbalance (relative dominance of the peroneus longus in the presence of a weak brevis) in the setting of chronic neurodegenerative disorders, may also be idiopathic and is not uncommon in athletes, who are at elevated risk for associated injury due to their activity level. In particular, hindfoot varus leads to lateral overload, placing the peroneal tendons, particularly the brevis, at increased risk for injury.<sup>10,38</sup>

*Plantar plates.* Hyperdorsiflexion injury to the plantar plate of the first MTP joint, colloquially termed “turf toe,” has been associated with the use of flexible cleated shoes, particularly on artificial turf. American football players are especially vulnerable to this type of injury when they are tackled, specifically when the tackling player lands on the back of the tackled player’s heel. Injury severity may range from low-grade ligamentous sprain to sesamoid fracture and MTP joint dislocation.<sup>14</sup> While injury to the first MTP joint often results from acute trauma incurred during athletic activity, pathology of the lesser plantar plates is typically related to degenerative processes and may be implicated as a cause of chronic metatarsalgia.<sup>33</sup>

The plantar plates are fibrocartilaginous structures that arise predominantly from the plantar capsule and plantar

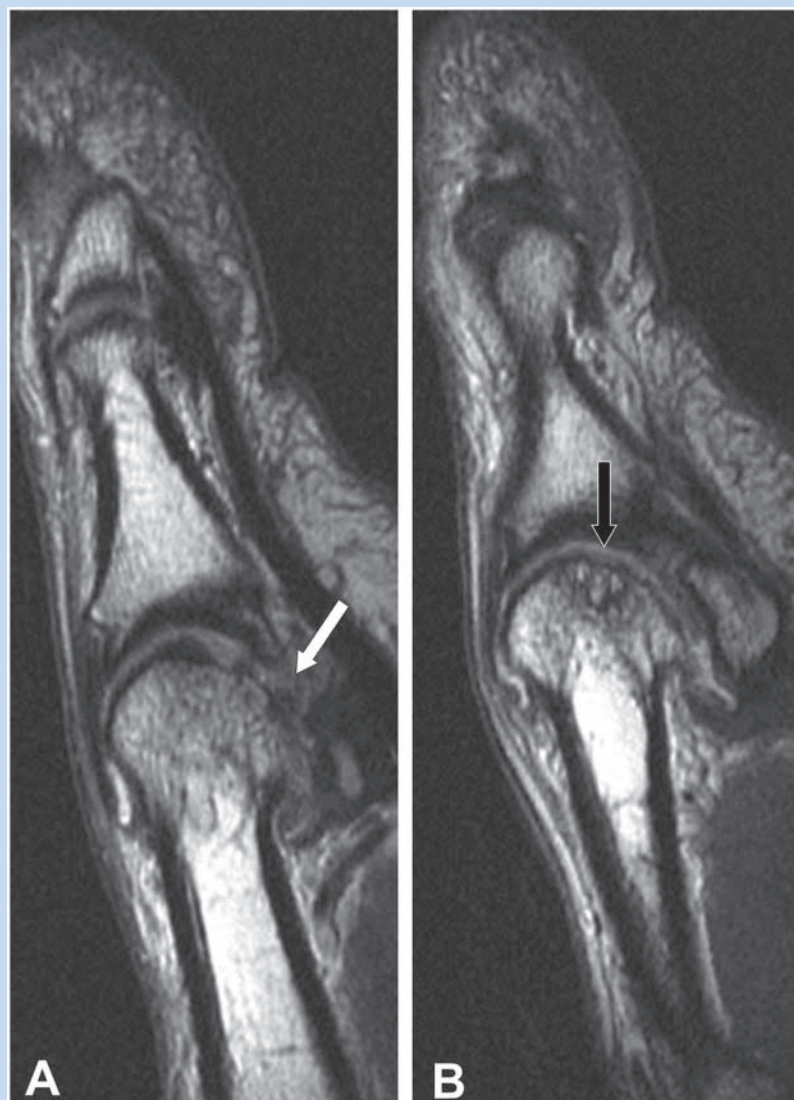


Figure 11. Twenty-eight-year-old running back with turf toe. Sagittal FSE images (A, B) demonstrate disruption of the plantar plate (white arrow) with associated chondral shear over the metatarsal head (black arrow).

aponeurosis of the MTP joints, serving a supportive function at the MTP joint and as a point of attachment for the multiple ligamentous and tendinous structures in the area. The plantar plate complex of the first MTP joint differs from that of the lesser digits in that it incorporates the hallux sesamoids in addition to the plantar capsule and plantar aponeurosis, whereas the lesser plantar plates, given the absence of sesamoids, span the interval between the metatarsal heads and proximal phalangeal bases without any intervening osseous structure.<sup>14,37</sup>

The plantar plates are best visualized in the sagittal plane; high-resolution thin sagittal images through the affected ray are useful for detailed evaluation of the complex anatomy about the MTP joints. The normal plantar plate is uniformly low in signal and is thickest distally, tapering proximally. Acute

plantar plate disruption at the first MTP joint may involve the osseous and fibrocartilaginous components of the plantar plate and may be associated with concurrent injury to the articular cartilage and adjacent tendons (Figure 11). Imaging findings include soft tissue edema and capsular disruption if the plantar plate complex fails at its ligamentous portion, typically at the distal pole of the sesamoid, or sesamoid fracture if the osseous component fails. Complete rupture may result in retraction of the sesamoids on weightbearing radiographs; comparison views of the contralateral foot are useful to assess for subtle changes in alignment. Associated flexor tendon injury, metatarsal fracture, and traumatic chondral shear may also be visualized.<sup>14</sup>

*Metatarsalgia.* Metatarsalgia is a generic term referring to chronic pain in the region of the metatarsal heads. Causes of

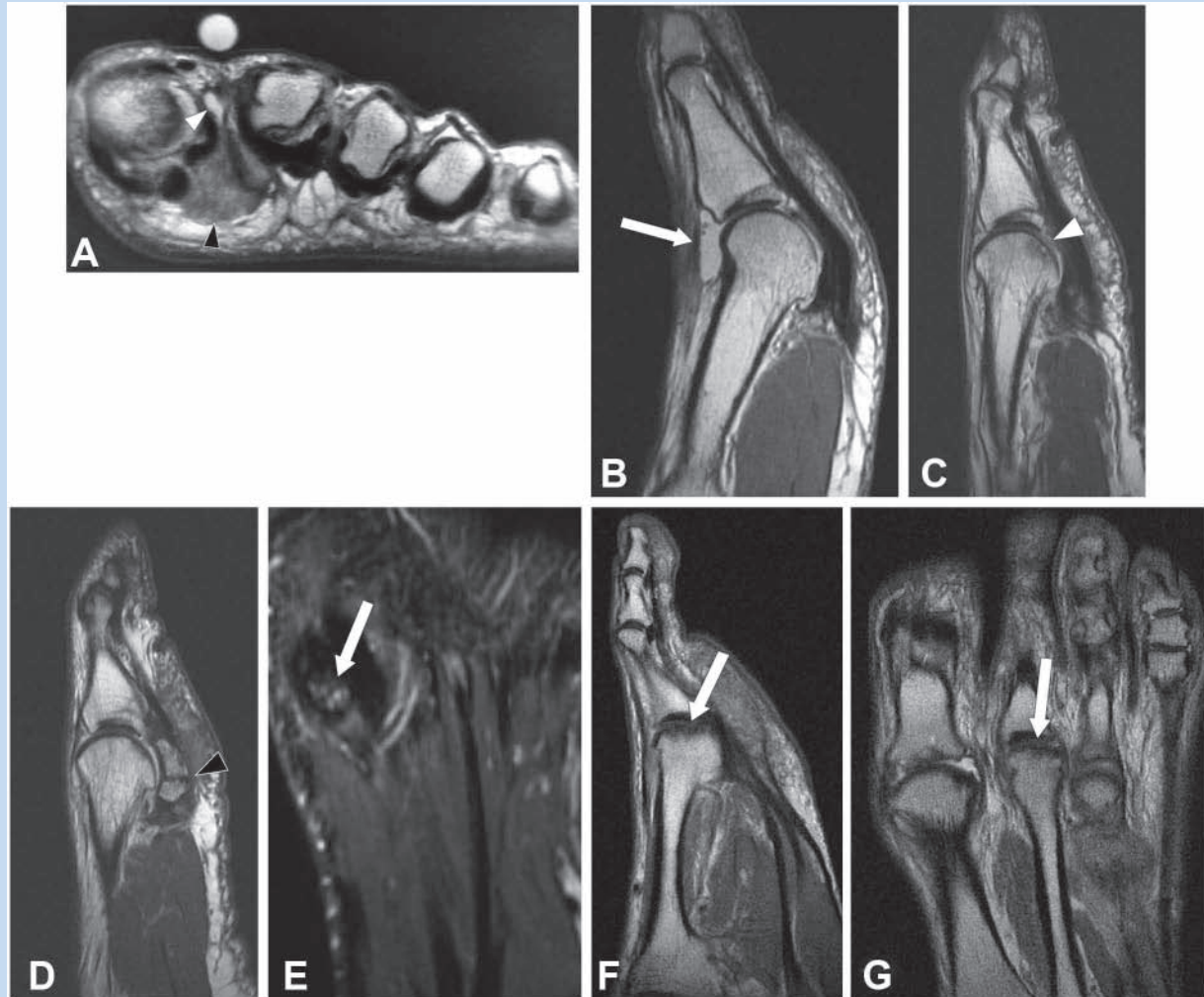


Figure 12. Common causes of metatarsalgia. Axial FSE image (A) in a 32-year-old runner demonstrates an intermediate signal intensity mass within the first webspace, consistent with an interdigital neuroma (black arrowhead); note adjacent fluid-distended intermetatarsal bursa (white arrowhead). Sagittal FSE image (B) in a 36-year-old dancer demonstrates synovitis of the first MTP joint (white arrow). Sagittal FSE images (C, D) in a 48-year-old golfer demonstrate subchondral impaction injury with chondral loss over the first metatarsal head (white arrow) and additional full-thickness cartilage loss over the partite medial sesamoid (black arrowhead), where there is also stress reaction about the synchondrosis (white arrow). Sagittal (E) and coronal (F) FSE images in a 29-year-old runner demonstrate flattening and sclerosis of the second metatarsal head (white arrows), consistent with Freiberg infraction.

metatarsalgia are generally related to chronic repetitive stress and include plantar plate injury (discussed above), metatarsal stress fracture (discussed below), Freiberg infraction (discussed below), interdigital neuromata, MTP synovitis, and osteoarthritis.<sup>14,28,33</sup>

Interdigital, also known as Morton, neuromata occur because of chronic friction upon the interdigital nerve related to the adjacent transverse intermetatarsal ligament, which results in perineural fibrosis, fibrinoid degeneration, demyelination, and endoneural fibrosis<sup>14</sup>; hence, the condition is not a true neuroma but rather a chronic entrapment neuropathy. On MRI, interdigital neuromata are best visualized in the axial plane and appear as intermediate signal intensity areas of focal fibrosis

within the intermetatarsal spaces, distal to the level of the intrinsic muscles of the foot. The second and third web spaces are most commonly affected, and an adjacent fluid-distended intermetatarsal bursa is not an uncommon finding (Figure 12A).<sup>14</sup>

MTP joint synovitis typically results from chronic compressive and tensile forces related to ambulation and may be exacerbated in cases of altered biomechanics, as may result from such conditions as hallux valgus or congenitally elongated second toe. High-heeled shoes with narrow toes tend to increase load upon the MTP joint and are an additional predisposing factor. Load tends to be greatest at the second MTP joint, which is therefore most commonly affected.

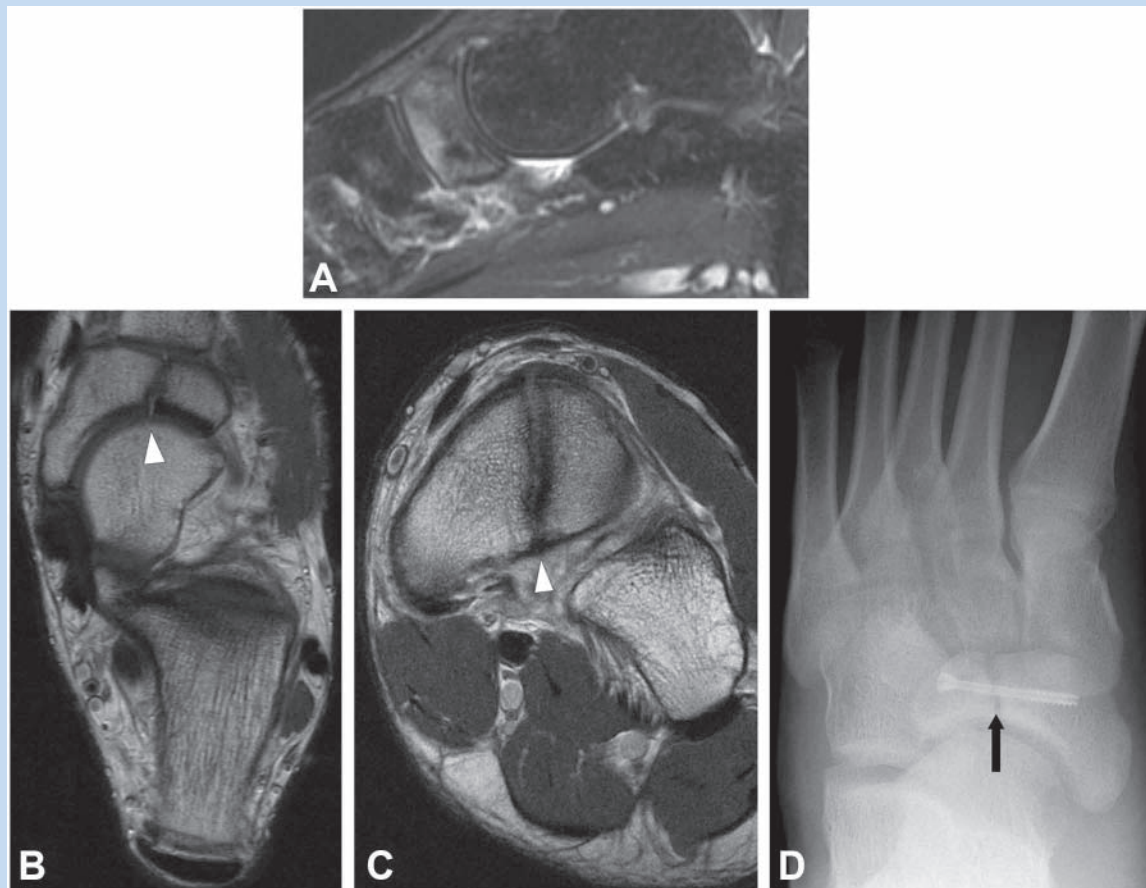


Figure 13. Twenty-one-year-old basketball player with nonunion of navicular stress fracture. Sagittal short tau inversion recovery (A) demonstrates marrow edema signal within the navicular. Coronal (B) and axial (C) FSE images demonstrate sagittally oriented fracture line with sclerotic margins, consistent with nonunion of navicular stress fracture (white arrowheads). Subsequent radiograph (D) demonstrates interval fixation of fracture (black arrow) with a single screw.

Imaging findings include synovitis at the MTP articulation; capsular distention due to synovial expansion may result in associated joint instability, which may lead to secondary degeneration of the plantar plate and collateral ligaments (Figure 12B).<sup>28,33</sup>

Degenerative arthrosis of the first MTP joint is a common condition in athletes who repeatedly stress the joint, typically in the setting of repetitive hyperdorsiflexion. Golfer's toe is a painful condition affecting the hallux MTP joint, related to hyperdorsiflexion at the first MTP joint of the rear foot during the golf swing. Stresses secondary to repetitive hyperdorsiflexion often result in degeneration of the articular surfaces of the MTP joint, as well as stress reaction within the hallux sesamoids, which may progress to osteonecrosis (Figure 12C-12E).<sup>26</sup> Similarly, in ballet dancers, repetitive hyperdorsiflexion often results in first MTP degeneration and hallux rigidus, with the resultant alteration in forefoot biomechanics predisposing the dancer to further injury.<sup>28</sup>

### Osseous Injury

Sports-related osseous injuries of the midfoot and forefoot may occur due to both acute and chronic causes. Acute fractures most commonly occur in the toes but may involve any location depending on the mechanism of injury. Chronic overload may lead to stress injuries; in the athlete, these are most commonly due to fatigue rather than osseous insufficiency. Stress injuries exist on a spectrum from low-grade stress reactions to complete stress fractures, which may progress to nonunion. Imaging findings are therefore variable; low-grade stress reactions manifest as focal marrow edema on MRI but tend to be occult on radiography. A frank stress fracture appears as a discrete linear low-signal abnormality with surrounding marrow edema and may be partial or complete. Complete stress fractures that progress to nonunion are characterized by sclerotic fracture margins and possible distraction or displacement on imaging.



Figure 14. Fractures of the fifth metatarsal base. Frontal radiograph (A) demonstrates fifth metatarsal base fractures based on location. Frontal radiograph (B) in a 24-year-old runner following inversion injury demonstrates an avulsion fracture of the fifth metatarsal base. Oblique radiograph (C) in an 11-year-old boy demonstrates an unfused fifth metatarsal base apophysis, a common fracture mimic.

**Navicular:** Navicular stress fractures are the third-most common lower extremity stress fracture, accounting for approximately 20% of all lower extremity stress fractures; they occur with less frequency than tibial stress fractures and with a similar frequency to metatarsal stress fractures. Stress fractures of the navicular are especially common in athletes, particularly in runners, in whom up to 60% of navicular stress fractures occur.<sup>2,19,35</sup>

Navicular stress fractures are typically oriented in the sagittal plane and are therefore most conspicuous on oblique coronal and axial images. They manifest as areas of marrow edema about a linear focus of low-signal intensity representing the fracture line and may be partial or complete. Complete fractures carry the additional risks of nonunion and osteonecrosis of the relatively poorly vascularized lateral segment. Lack of healing in combination with sclerotic fracture margins implies nonunion, while osteonecrosis manifests as edema and/or sclerosis within the affected fragment; bone that is nonviable appears uniformly hypointense on all magnetic resonance sequences (Figure 13).<sup>2,19,35</sup> Computed tomography, given its superior depiction of osseous detail,

provides sensitive depiction of subtle foci of lucency and sclerosis, aiding differentiation of stress reaction, fracture, and osteonecrosis.

**Metatarsal.** Injury to the metatarsals is common in both acute and chronic settings. Metatarsal stress fractures are a common occurrence in athletes, particularly in runners, in whom they account for 20% of lower extremity stress fractures. Given the increased stresses experienced by the second and third metatarsals during walking and running, these metatarsals are at greatest risk for stress fracture.<sup>2,35</sup>

Fractures of the fifth metatarsal base may be categorized as avulsion, Jones, and stress fractures. Each fracture has a characteristic location (Figure 14A). Avulsion fracture involves the tip of the styloid process at the attachment of the plantar aponeurosis and peroneus brevis (Figure 14B). A Jones fracture occurs approximately 1.5 cm distally, secondary to dorsiflexion with the foot in supination. Fractures of the midshaft are generally fatigue fractures related to chronic stress.<sup>19</sup> A common fracture mimic in this region is the unfused fifth metatarsal base apophysis, which is typically present in 9- to 14-year-olds; unlike

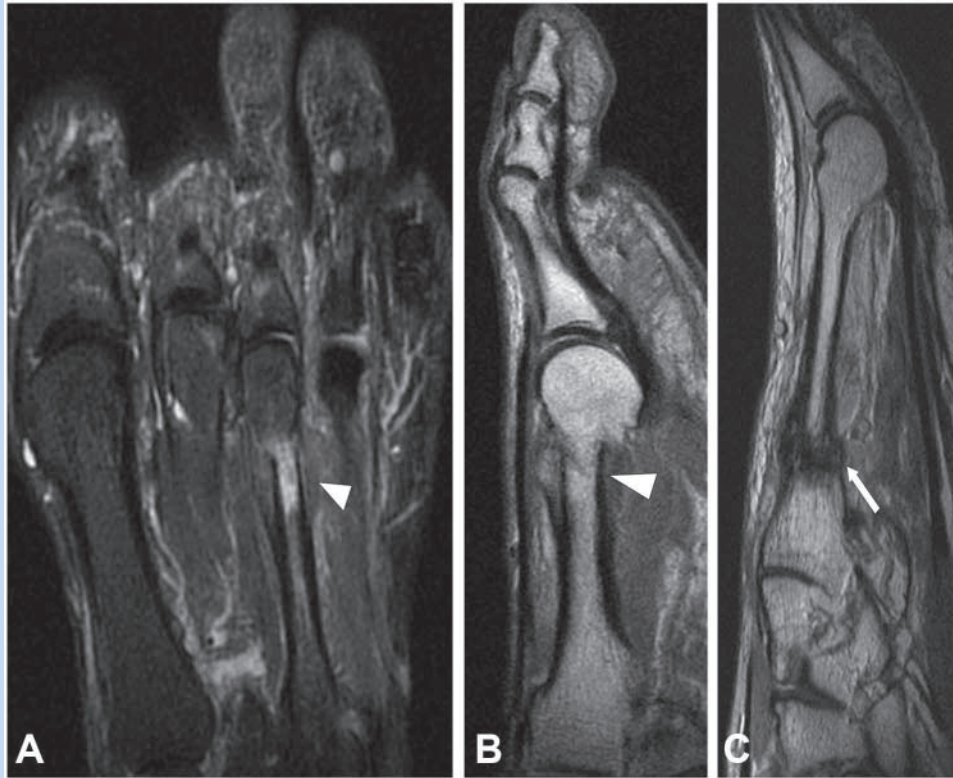


Figure 15. Metatarsal stress fractures. Coronal short tau inversion recovery (A) and sagittal FSE (B) images in a 33-year-old runner demonstrate marrow edema with a low-signal incomplete fracture line and associated periosteal reaction (white arrowheads) within the distal third metatarsal shaft, consistent with incomplete stress fracture. Sagittal FSE image (C) in a 42-year-old runner demonstrates stress fracture of the proximal second metatarsal shaft with sclerotic margins, consistent with nonunion (white arrow).

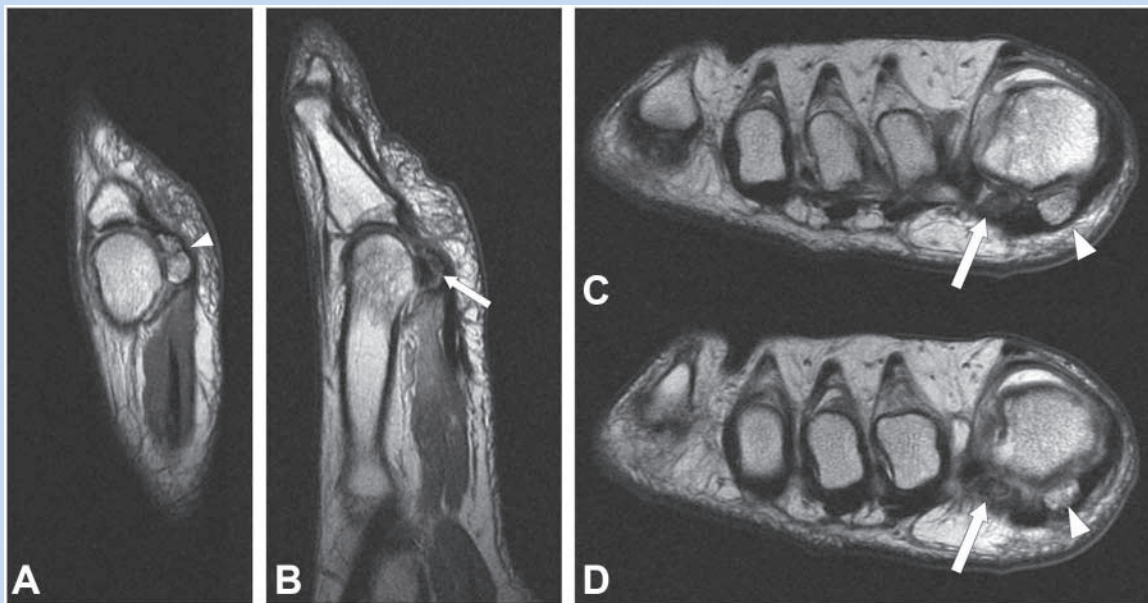


Figure 16. Forty-year-old runner with sesamoid injury. Sagittal (A, B) and axial (C, D) FSE images of the forefoot demonstrate nonunion of medial sesamoid stress fracture (white arrowheads) and avascular necrosis of lateral sesamoid (white arrows).

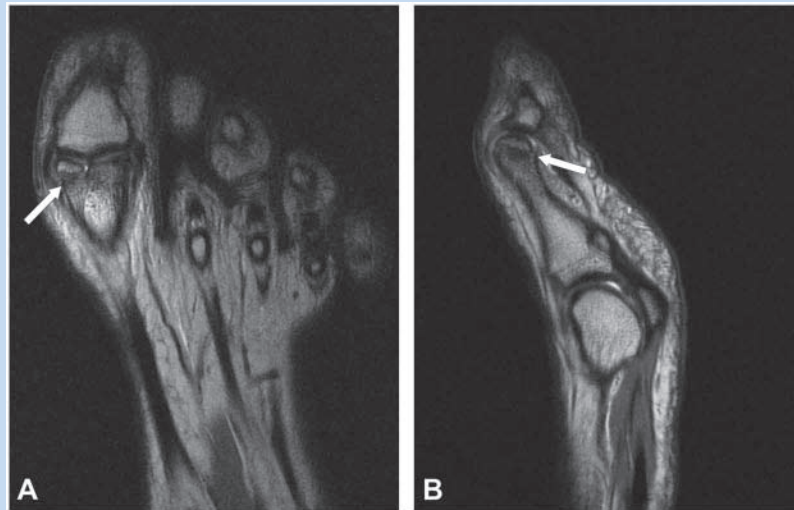


Figure 17. Fourteen-year-old soccer player with fracture of proximal phalanx. Coronal (A) and sagittal (B) FSE images demonstrate subacute intra-articular fracture of the distal first proximal phalanx (white arrow).



Figure 18. Forty-one-year-old runner with chondral shear. Sagittal (A) and axial (B) images demonstrate chondral shear over the medial sesamoid (white arrows).

fractures which occur in this area, the lucent line associated with an unfused apophysis is always longitudinally oriented (Figure 14C), and comparison radiographs of the contralateral foot are helpful in equivocal cases.

On radiographs, stress reaction will commonly be occult, while stress fractures may appear as areas of focal periosteal reaction with or without a visible discrete fracture line. On MRI, stress reactions manifest as varying degrees of marrow edema, while a discrete fracture line will be evident in the

setting of a frank stress fracture. If complete, the fracture is at risk for nonunion (Figure 15A-15C).<sup>35</sup>

*Sesamoids.* Injuries of the hallux sesamoids constitute 1% of all running injuries; the majority of these injuries are related to chronic repetitive stress, while the acute traumatic injury is relatively rare.<sup>3,4</sup> Activities involving running, jumping, and repeated passive dorsiflexion are associated with a greater risk of sesamoid injury. Golfers, as described above, are vulnerable

to sesamoid injury because of repetitive hyperdorsiflexion of the hallux MTP joint.<sup>3,26</sup>

Blood supply to the hallux sesamoids is primarily extraosseous, originating from the proximal and plantar directions via the proper plantar and first plantar metatarsal arteries. For this reason, the sesamoids are particularly vulnerable to ischemia and osteonecrosis following injury.<sup>4</sup>

The hallux sesamoids are well assessed in the axial and sagittal planes. Imaging manifestations of sesamoid injury depend on the nature of pathology and commonly overlap. Sesamoid stress reaction and sesamoiditis both manifest as hyperintense signal on fluid sensitive images, though sesamoiditis more commonly involves both sesamoids and may have associated findings of tenosynovitis, tendinosis, and bursitis. Fractures of the sesamoids commonly involve the tibial sesamoid and may be visible as transversely oriented lucent fracture lines on radiographs. On MRI, the low-intensity fracture line is surrounded by marrow edema signal. Fractures complicated by nonunion possess sclerotic fracture margins, while those complicated by osteonecrosis display mixed edema and sclerosis or hypointense signal on all pulse sequences if nonviable (Figure 16A-16D).<sup>14,30,35</sup>

**Phalanges.** Stress fractures of the phalanges are relatively rare but have been reported in runners, volleyball players, and soccer players. Acute phalangeal fractures, however, are common injuries that tend to occur during running/push-off injury, stubbing injury, and crush injury (Figure 17).

Displaced fractures are generally evident on radiographs, while subtle nondisplaced fractures may be radiographically occult. On magnetic resonance, focal marrow edema signal in a patient with a history of injury, and negative radiographs should prompt a search for a fracture line. Stress injury may be radiographically subtle or occult; for example, low-grade stress reaction manifests as focal marrow edema on MRI, often without associated radiographic findings.<sup>19</sup>

**Osteochondral/chondral injury.** Acute traumatic chondral or osteochondral injury often occurs in conjunction with other injuries of the foot. For example, shear forces sustained during a hyperdorsiflexion event leading to a turf toe injury commonly result in associated traumatic chondral shear over the first metatarsal head. Direct impaction injury, such as a jammed digit, may result in osteochondral injury of the metatarsal head (Figure 18).

Freiberg infraction is an osteonecrosis of the metatarsal head, the etiology of which remains controversial. The exact pathogenesis is likely multifactorial, involving a confluence of vascular and traumatic insults; young women who are active in sports appear to be at elevated risk for the condition. Radiographs demonstrate flattening and sclerosis of the metatarsal head, with the second metatarsal head being the most commonly affected. In addition to metatarsal head flattening and sclerosis, MRI demonstrates associated marrow edema and chondral injury and also has the ability to detect radiographically occult lesions (Figure 12F and 12G).<sup>14,28</sup>

## CONCLUSION

The foot is at risk for a variety of acute and chronic sports-related injuries, largely due to the shifting loads and stresses that it experiences during athletic activity. Given the complex anatomy of the foot, as well as the fact that injuries in this region often involve soft tissue structures, MRI is an optimal imaging examination for evaluation of suspected foot injury, though radiographic evaluation is often an appropriate initial step. Evaluation is complemented by computed tomography, which provides superior osseous detail, as well as ultrasound and fluoroscopy, which provide dynamic imaging capabilities. Familiarity with injury mechanism, risk factors, and clinical presentation benefits the radiologist in elevating the index of suspicion for commonly associated patterns of injury, facilitating accurate and timely diagnosis.

## REFERENCES

- Adelaar RS. Complications of forefoot and midfoot fractures. *Clin Orthop Relat Res.* 2001;391:26-32.
- Anderson RB, Hunt KJ, McCormick JJ. Management of common sports-related injuries about the foot and ankle. *J Am Acad Orthop Surg.* 2010;18(9):546-556.
- Boike A, Schnirring-Judge M, McMillin S. Sesamoid disorders of the first metatarsophalangeal joint. *Clin Podiatr Med Surg.* 2011;28(2):269-285.
- Cohen BE. Hallux sesamoid disorders. *Foot Ankle Clin.* 2009;14(1):91-104.
- Conti SF. Posterior tibial tendon problems in athletes. *Orthop Clin North Am.* 1994;25(1):109-121.
- Crim J. MR imaging evaluation of subtle Lisfranc injuries: the midfoot sprain. *Magn Reson Imaging Clin N Am.* 2008;16(1):19-27.
- Deland JT. Adult-acquired flatfoot deformity. *J Am Acad Orthop Surg.* 2008;16(7):399-406.
- DeLee JC, Farney WC. Incidence of injury in Texas high school football. *Am J Sports Med.* 1992;20(5):575-580.
- Desai KR, Beltran LS, Bencardino JT, Rosenberg ZS, Petchprapa C, Steiner G. The spring ligament recess of the talocalcaneonavicular joint: depiction on MR images with cadaveric and histologic correlation. *AJR Am J Roentgenol.* 2011;196(5):1145-1150.
- Desai SN, Grierson R, Manoli A. The cavus foot in athletes: fundamentals of examination and treatment. *Oper Tech Sports Med.* 2010;18:27-33.
- Desmond EA, Chou LB. Current concepts review: Lisfranc injuries. *Foot Ankle Int.* 2006;27(8):653-660.
- Garrick JG, Requa RK. The epidemiology of foot and ankle injuries in sports. *Clin Sports Med.* 1988;7(1):29-36.
- Hatem SF. Imaging of lisfranc injury and midfoot sprain. *Radiol Clin North Am.* 2008;46(6):1045-1060.
- Hockenbury RT. Forefoot problems in athletes. *Med Sci Sports Exerc.* 1999;31(7):S448-S458.
- Kavanagh EC, Zoga AC. MRI of trauma to the foot and ankle. *Semin Musculoskelet Radiol.* 2006;10(4):308-327.
- Khouri V, Guillin R, Dhanju J, Cardinal E. Ultrasound of ankle and foot: overuse and sports injuries. *Semin Musculoskelet Radiol.* 2007;11(2):149-161.
- Lattermann C, Goldstein JL, Wukich DK, Lee S, Bach BR Jr. Practical management of Lisfranc injuries in athletes. *Clin J Sport Med.* 2007;17(4):311-315.
- Lo LD, Schweitzer ME, Fan JK, Wapner KL, Hecht PJ. MR imaging findings of entrapment of the flexor hallucis longus tendon. *AJR Am J Roentgenol.* 2001;176(5):1145-1148.
- Mandraccchia VJ, Mandi DM, Toney PA, Halligan JB, Nickles WA. Fractures of the forefoot. *Clin Podiatr Med Surg.* 2006;23(2):283-301.
- Melao L, Canella C, Weber M, Negro P, Trudell D, Resnick D. Ligaments of the transverse tarsal joint complex: MRI-anatomic correlation in cadavers. *AJR Am J Roentgenol.* 2009;193(3):662-671.
- Mengiardi B, Pfirrmann CW, Vienne P, et al. Anterior tibial tendon abnormalities: MR imaging findings. *Radiology.* 2005;235(3):977-984.
- Mengiardi B, Pfirrmann CW, Zanetti M. MR imaging of tendons and ligaments of the midfoot. *Semin Musculoskelet Radiol.* 2005;9(3):187-198.



23. Mengiardi B, Zanetti M, Schottle PB, et al. Spring ligament complex: MR imaging-anatomic correlation and findings in asymptomatic subjects. *Radiology*. 2005;237(1):242-249.
24. Myerson MS, Fisher RT, Burgess AR, Kenzora JE. Fracture dislocations of the tarsometatarsal joints: end results correlated with pathology and treatment. *Foot Ankle*. 1986;6(5):225-242.
25. Orendurff MS, Rohr ES, Segal AD, Medley JW, Green JR 3rd, Kadel NJ. Regional foot pressure during running, cutting, jumping, and landing. *Am J Sports Med*. 2008;36(3):566-571.
26. Petrella RJ, Cogliano A. Intra-articular hyaluronic acid treatment for golfer's toe: keeping older golfers on course. *Phys Sportsmed*. 2004;32(7):41-45.
27. Potter HG, Deland JT, Gusmer PB, Carson E, Warren RF. Magnetic resonance imaging of the Lisfranc ligament of the foot. *Foot Ankle Int*. 1998;19(7):438-446.
28. Prisk VR, O'Loughlin PF, Kennedy JG. Forefoot injuries in dancers. *Clin Sports Med*. 2008;27(2):305-320.
29. Raikin SM, Elias I, Dheer S, Besser MP, Morrison WB, Zoga AC. Prediction of midfoot instability in the subtle Lisfranc injury: comparison of magnetic resonance imaging with intraoperative findings. *J Bone Joint Surg Am*. 2009;91(4):892-899.
30. Riley GM. Magnetic resonance imaging in the evaluation of sports injuries of the foot and ankle: a pictorial essay. *J Am Podiatr Med Assoc*. 2007;97(1):59-67.
31. Sherman KP. The foot in sport. *Br J Sports Med*. 1999;33(1):6-13.
32. Ting AY, Morrison WB, Kavanagh EC. MR imaging of midfoot injury. *Magn Reson Imaging Clin N Am*. 2008;16(1):105-115.
33. Umans HR. Imaging sports medicine injuries of the foot and toes. *Clin Sports Med*. 2006;25(4):763-780.
34. Vormittag K, Calonje R, Briner WW. Foot and ankle injuries in the barefoot sports. *Curr Sports Med Rep*. 2009;8(5):262-266.
35. Wall J, Feller JF. Imaging of stress fractures in runners. *Clin Sports Med*. 2006;25(4):781-802.
36. Watson TS, Shurnas PS, Denker J. Treatment of Lisfranc joint injury: current concepts. *J Am Acad Orthop Surg*. 2010;18(12):718-728.
37. Yao L, Do HM, Cracchiolo A, Farahani K. Plantar plate of the foot: findings on conventional arthrography and MR imaging. *AJR Am J Roentgenol*. 1994;163(3):641-644.
38. Younger AS, Hansen ST Jr. Adult cavovarus foot. *J Am Acad Orthop Surg*. 2005;13(5):302-315.

For reprints and permission queries, please visit SAGE's Web site at <http://www.sagepub.com/journalsPermissions.nav>.